Intermolecular structure and hydrogen-bonding in liquid 1,2-propylene carbonate and 1,2-glycerol carbonate determined from neutron scattering

Intermolecular structure and hydrogen-bonding in liquid 1,2-propylene carbonate and 1,2-glycerol carbonate determined from neutron scattering†

Yoan M. Delavoux, Mark Gilmore, Martin P. Atkins, Małgorzata Swadźba-Kwaśny and John D. Holbrey*

Neutron diffraction with isotopic substitution has been used to investigate the liquid structures of propylene carbonate and glycerol carbonate. C-H···O=C hydrogen-bonding motifs dominate the local structure of propylene carbonate, giving rise to the formation of head-to-tail correlated chains of molecules. In contrast, glycerol carbonate exhibits a more disordered structure with no overall dominant interactions in which the pendant hydroxyl function disrupts structure-making correlations present in propylene carbonate.

Introduction

The small organic carbonates have many uses, especially as solvents.[1,2] They are typically colourless, relatively polar, aprotic fluids with wide liquid ranges, low ecotoxicity, and good biodegradability. Propylene carbonate is used as a component in electrolyte solutions for lithium ion batteries. It has a liquid range of nearly 200 °C (mp -55 °C, bp 240 °C), high molecular dipole moment of 4.9 D (*cf.* 2.91 D for acetone and 1.78 D for ethyl acetate), a large dielectric constant[3] of *ca.* 64, partial miscibility with water (250 g dm^{-3} at 25 °C), and wide electrochemical window. It readily dissolves alkali metal salts, and such solutions find uses as electrolytes with high ionic conductivity.[4]

Both glycerol carbonate[5] and propylene carbonate are good solvents for many inorganic salts.[6] The two liquids differ by the presence of the terminal hydroxyl group which gives glycerol carbonate (1) a higher dielectric constant (109.7)[6] and complete miscibility with water. The Hildebrand (δ) and hydrogen-bonding component of the Hansen solubility parameters for glycerol carbonate closer to those of glycerol and water than those for propylene carbonate. This reflects the importance of the hydroxyl group. In contrast, both the dispersive and polar terms from the Hansen solubility parameter more closely resemble

QUILL, School of Chemistry and Chemical Engineering, The Queen's University of Belfast, Belfast, BT9 5AG, Northern Ireland. Tel: +44 (0) 28 9097 4836; E-mail: j.holbrey@qub.ac.uk

† Electronic Supplementary Information (ESI): C/O centred partial radial distribution functions and centre of mass spatial density function maps calculated for propylene carbonate and glycerol carbonate

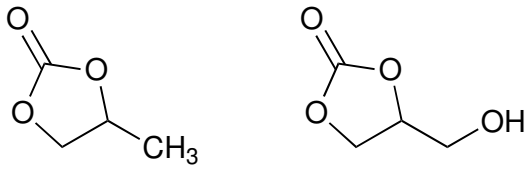

Fig. 1 Structures of propylene carbonate and glycerol carbonate.

those of other alkylene carbonates than water or glycerol. Consequently, glycerol carbonate exhibits the polarity of cyclic alkylene carbonates (comparable to propylene carbonate) while having the proticity of glycerol.[7,8]

As a chemical intermediate, glycerol carbonate has a key role in the valorisation of bio-glycerol[5,9] generated from fatty acid methyl ester biodiesel production. In this context, glycerol can be easily converted to glycerol carbonate by base-catalysed transesterification reactions with dimethyl carbonate.[10] Glycerol carbonate has application as a more stable, thus better storable and transportable alternative to 2,3-epoxypropanol (glycidol), used in the synthesis of polyglycerols through ring-opening[11] or anionic polymerisation.[12] Similarly, it can be used as both reagent and blowing agent to produce polyurethane foams.[13]

Schaeffner *et al.*[2] have proposed the use of glycerol carbonate as a low volatility general-purpose alternative to toxic VOCs such as N-methyl pyrrolidone, methylene chloride, or dimethyl formamide, taking advantage of its high boiling point, low vapour pressure and low toxicity. In this vein, enzymatic biocatalysis in non-aqueous environment has recently been investigated.[14] Transesterification reactions using *Candida antarctica* lipase B and *Candida rugosa* lipase were compared in water and glycerol carbonate. Enzymes dissolved in glycerol carbonate showed constant activity after storage for four weeks, suggesting that it could be an effective non-aqueous solvent for biocatalysis. It was assumed that the presence of the hydroxyl group resulted in proticity resembling that of glycerol, with 'water-like' characteristics[15] that support biocompatibility and activity.

The structure of liquid propylene carbonate has not previously been studied using neutron diffraction. Propylene carbonate have been investigated by Soetens *et al.*[16] and by Eckstein *et al.*[17] using MD simulation combined with experimental data from X-ray diffraction. Eckstein *et al.* examined the structural dynamics of propylene carbonate as a glass forming liquid and interpreted their results in terms of the formation of cluster-like heterogeneities in the liquid as the glass transition temperature, 160 K, was approached. A significant degrees of parallel orientation of the molecular planes was identified even at 290 K by calculating a distance dependent orientation pair correlation function, $S(r,\psi)$. However, no molecular interpretation of the results was presented.

Wang and Balbuena[18] identified intermolecular C-H···O interactions as the main mode of association between cyclic carbonate molecules using *ab initio* and density functional theory methods. Silva and Freitas[19] used pure Monte Carlo simulations to explore the

Table 1 Isotopomers of propylene carbonate and glycerol carbonate investigated

Sample	Sample Name	Empirical formula
Propylene carbonate		
1	H	$C_3O_3H_6$
2	H/D[a]	$C_3O_3(H/D)_6$
3	D	$C_3O_3D_6$
Glycerol carbonate		
4	H	$C_3O_3H_5OH$
5	H/D[a]	$C_3O_3(H/D)_5O(H/D)$
6	D	$C_3O_3D_5OD$
7	D_1	$C_3O_3H_5OD$
8	D_5	$C_3O_3D_5OH$

[a] 1:1 H:D isotopic substitution.

bulk liquid structures of propylene carbonate and ethylene carbonate, and more recently, a number of classical and *ab initio* studies[20] in relation to lithium ion battery applications have been made. The solvation environment of Li^+ ions dissolved in propylene carbonate has been studied using time of flight neutron spectroscopy[21] using $^6Li/^7Li$ isotopic substitution. It is worth noting that propylene carbonate is not a good solvent for lithium batteries (*cf.* ethylene carbonate) due to the tendency to induce exfoliation of graphite electrodes. The differences between propylene carbonate and ethylene carbonate intercalated into graphene sheets has also been investigated computationally[22] with a view to designing new anode materials.

Although the primary association interactions that may be present in liquid propylene carbonate, namely C-H···O interactions, have been identified *in silico*[18,19] this information has not been fully integrated into an atomistic description of the bulk liquid structure based on experimental data. Similarly, to the best of our knowledge, the structure of glycerol carbonate has not been investigated using either experimental X-ray or neutron diffraction or by computational methods. Nagumo *et al.*[23] have used MD simulations to predict CO_2 solubilities in a range of solvents, including glycerol carbonate, but did not study the solvent structure.

Given the interest in glycerol carbonate as a bio-sourced solvent,[5,9] it is important to have a good understanding of the structure of the liquid, and also how it relates to that of glycerol and propylene carbonate. The lack of experimental data, and current interest in glycerol carbonate, suggest the need for systematic experimental investigation of the liquid structure. In this work, we apply total neutron scattering with isotopic substitution to investigate the structure of two cyclic carbonates: propylene carbonate and glycerol carbonate. We aim to identify the differences, induced by the presence of the hydroxyl group in glycerol carbonate, and understand their influence on the differing solvent properties of both carbonates.

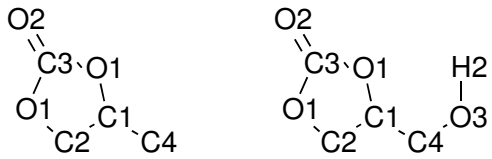

Fig. 2 Atom labels used to define unique atom types in the initial EPSR simulation models for propylene carbonate (left) and glycerol carbonate (right). All hydrogen atoms attached to carbons were defined as H1.

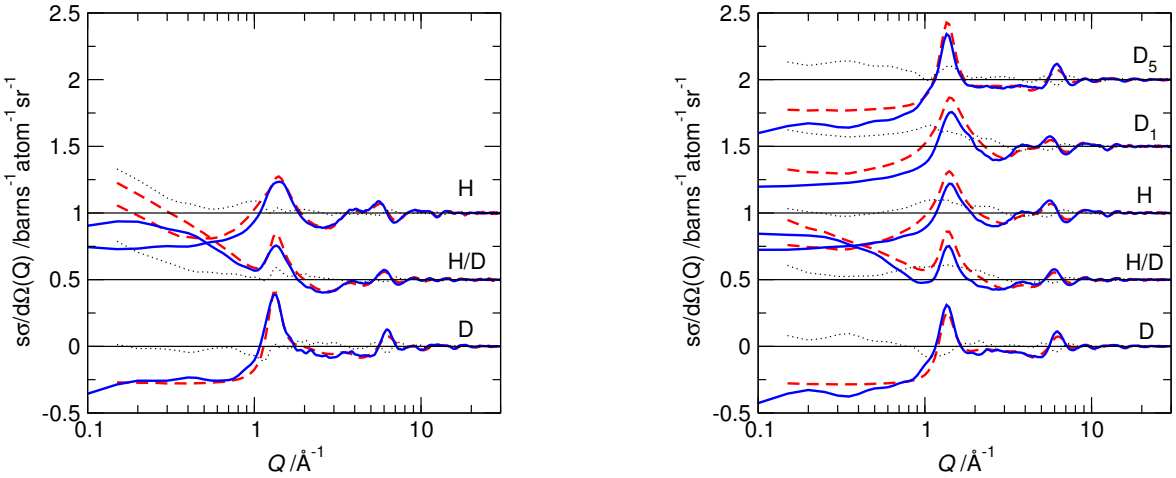

Fig. 3 Experimental S(Q) data (dashed lines), EPSR models for the data (solid lines) and residual differences between simulated and experimental data (dotted lines) for propylene carbonate (left) and glycerol carbonate (right). Labels represent the experimental compositions shown in Table 1.

Experimental

Propylene carbonate and glycerol were purchased from Sigma-Aldrich. Deuteriated propylene carbonate-d_6 and deuteriated glycerol-d_6 were purchased from Cambridge Isotopes (Goss Scientific Instruments Ltd, Crewe, UK). Three H/D-isotopologs of propylene carbonate (fully-protiated, fully-deuteriated, and a 1:1 mixture) and five of glycerol carbonate (fully-protiated, fully-deuteriated, 1:1 mixture, and two alcohol-site H/D-contrasted samples) were prepared and studied (Table 1). Protiated glycerol carbonate-h_6 and fully deuteriated glycerol carbonate-d_6 were prepared by base-catalysed reaction of glycerol with dimethyl carbonate, adapting the method described by Rokicki *et al.*[24] to use with deuteriated reagents as appropriate. Residual catalyst was removed from the resultant basic glycerol carbonates by neutralisation, using an acidic (H^+–form) Amberlite IR120 cation exchange resin. The protiated alcohol group of glycerol carbonate-d_5 (D_5 in Table 1) produced after neutralisation, was H/D exchanged to give the fully deuteriated glycerol carbonate-d_6 by repeated freeze-thaw mixing and evaporation with D_2O (3×2 volumes). Glycerol carbonate-d_1 was prepared in the same manner by repeated evaporation of D_2O

Table 2 Lennard-Jones well depth (ε), range (σ), and charge (q) parameters used for the reference potential of the Empirical Potential Structure Refinement model.

Atom label	ε /kJ mol^{-1}	σ /Å	q /e
Propylene carbonate			
C1	0.800	3.70	0.00040
C2	0.800	3.70	0.39250
C3	0.800	3.70	-0.05390
C4	0.800	3.70	-0.22910
H1	0.000	0.00	0.10923
O1	0.650	3.10	-0.24445
O2	0.650	3.10	-0.27650
Glycerol carbonate			
C1	0.800	3.70	-0.00370
C2	0.800	3.70	-0.03655
C3	0.800	3.70	0.39040
C4	0.800	3.70	-0.03655
H1	0.000	0.00	0.11414
H2	0.000	0.00	0.21400
O1	0.650	3.10	-0.24445
O2	0.650	3.10	-0.27420
O3	0.650	3.10	-0.33540

from glycerol carbonate-h_6. IR spectroscopy and MS were used confirm the extent of deuteriation and OH/OD exchange.

Densities of all the materials were measured using an Anton Paar DMA 4500 densitometer giving densities consistent with literature values for the protiated materials (propylene carbonate, 1.20 g cm^3 and glycerol carbonate, 1.40 g cm^3 at 25 °C). Elemental compositions, degree of isotopic substitution and atomic number densities were also consistent with the observed total neutron scattering cross sections for each sample in the SANDALS experiments.

Neutron scattering data were collected on eight samples (Table 1) using the SANDALS spectrometer at the ISIS pulsed neutron and muon source at the Rutherford Appleton Laboratory, UK. The instrument has a wavelength range of 0.05–4.5 Å, and data were collected over a Q range from 0.05–50 Å^{-1}. Each sample was contained in 'null scattering' $Ti_{0.68}Zr_{0.32}$ flat plate cells with internal geometries of $1 \times 35 \times 35$ mm, with a wall thickness of 1 mm. During measurements, the cell was maintained at a temperature of 298 K using a recirculating heater (Julabo FP50). Measurements were made on each of the empty sample holders, the empty spectrometer, and a 3.1 mm thick vanadium standard sample for the purposes of instrument calibration and data normalisation.

Data reduction was performed using GUDRUN,[25] to produce a differential scattering

Table 3 Intramolecular bond distance (Å) and non-hydrogen bond-angle (°) constraints used to define the basic geometries of propylene carbonate and glycerol carbonate in the initial EPSR simulation model.

Bond Distance /Å		Bond Angle / °	
Propylene carbonate			
C1-C2	1.539	O1–C1–C2	103.93
C1-C4	1.508	C2–C1–C4	113.62
C1-O1	1.451	C1–O1–C3	110.11
C1-H1	1.122	C1–C2–O1	104.84
C2-O1	1.442	O1–C3–O2	124.40
C2-H1	1.117	O1–C3–O1	111.16
C3-O1	1.369	C3–O1–C2	109.96
C3-O2	1.215		
C4-H1	1.117		
Glycerol carbonate			
C1-C2	1.532	C2–C1–O1	105.15
C1-C4	1.532	C2–C1–C4	114.04
C1-O1	1.448	C4–C1–O1	105.15
C1-H1	1.119	C1–C2–O1	104.23
C2-O1	1.443	O1–C3–O1	111.37
C2-H1	1.119	O1–C3–O2	124.30
C3-O1	1.373	C1–C4–O3	105.87
C3-O2	1.215	C1–O1–C3	109.14
C4-O3	1.420	C2–O1–C3	110.10
C4-H1	1.119	C4–O3–H2	106.67
O3-H2	0.964		

cross section for each experimental sample. The experimental sample densities and scattering levels were consistent with the actual isotopic compositions of the samples. Calibration and background subtraction for single atom scattering was made to produce a differential scattering cross section for each sample. Data from the neutron diffraction experiments was analysed using the Empirical Potential Structure Refinement (EPSR) program.[26,27] The experimental total structure factors, F(Q), were extracted from the neutron scattering data for each of the isotopically distinct samples at each composition. These were used to build and refine three dimensional models of the liquid structure consistent with the experimental data using EPSR for the two pure liquids (propylene carbonate and glycerol carbonate). The EPSR approach consists of a Monte Carlo simulation, using Lennard-Jones potentials with atom-centred point charges that are combined with basic information about the structure of the atoms or molecules present in the system and total atomic densities of the system to constrain the model in a chemically and physically reliable manner. By comparing the differences between calculated and experimental structure factors in Q-space

for data sets, an empirical perturbation potential is determined. This is combined with the reference potential used as the new potential for simulations, iteratively driving the simulation model towards agreement with experimental data.

All the EPSR simulation models were refined against the experimental data over the full data range (Q = 0.1–50 Å^{-1}). Within the EPSR simulations, initial potentials and interatomic distance constraints used to define the basic molecular geometries were obtained from MOPAC with the AM1 model. Atom types in each system were defined based on their unique positions in the molecular skeletons, as shown in Figure 2, and full rotational flexibility was enabled in the model. The full parameters of the reference potential used are given in Table 2 and the interatomic distance and angular constraints used to define the basic molecular geometries are summarised in Table 3.

Simulations were equilibrated over *ca.* 10000 cycles before accumulating and averaging data. The EPSR refinements were initialised using an equilibrated Monte Carlo simulation containing 1000 molecules as a a racemic mixture of *R*- and *S*-isomers in a cubic box of size 59.92 Å (glycerol carbonate) or 52.08 Å (propylene carbonate). The total numeric density of the simulation box corresponded to the experimentally determined molecular densities of the fully protiated materials. Centre of mass radial distribution functions were calculated using the SHARM routines within EPSR.

Chain correlation lengths were calculated using the 'chain' distribution routine in ESPR for C=O···propylene associations. Distance limits of 3.50, 3.75 and 4.00 Å were defined for the C=O···C2/4 distance to track through the first peak in the O2···C2 and O2···C4 site-site pRDFs (in Figure 5). The average number of bonds per molecule contribution to chains and the chain length are calculated based on linked paths between valid molecules with appropriate C=O···C2/4 distance correlations, counting only one path per molecule, and terminating chains with molecules that only have one link.

Results and Discussion

Neutron diffraction data were collected from samples of the three propylene carbonate and five glycerol carbonate isotopologues, described in Table 1. The liquid structures of the two cyclic carbonates were modelled using EPSR. In each case good, self-consistent fits were obtained between the experimental and EPSR-simulated structure factors. Each simulation model contained racemic mixtures of the *R*- and *S*-enantiomers of propylene carbonate or glycerol carbonate. Figure 3 shows comparisons of experimental and simulated S(Q) data for each of the experimental samples. Good agreement between the experimental data and the EPSR derived model across the Q-range of interest were obtained, which indicates consistency of the simulation model with the measured system. Some discrepancies were observed in the low Q region between the experimental and simulated data sets for hydrogen-rich samples. This was caused by the difficulties in removing the effect of inelastic scattering contributions from the measured data.

From the resulting simulation models, radial distribution functions (RDFs) from the

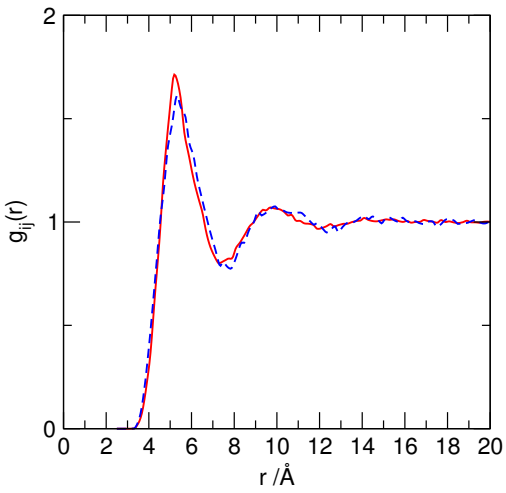

Fig. 4 Centre of mass RDFs for propylene carbonate (solid) and glycerol carbonate (dashed) showing the first correlation shell maximum at 5.3 Å.

centres of mass (Figure 4) were calculated. The centre-of-mass RDFs for both cyclic carbonates have very similar profiles (Figure 4), with a well-defined first coordination shell, featuring a maximum at 5.3 Å in and a first minimum at 7.6 Å. The second shell is apparent in both systems as a much more diffuse peak between 7.5–12.2 Å. Comparing the two RDFs, the first shell maximum for glycerol carbonate is slightly less intense and slightly broader than that of propylene carbonate, however this may be due to the small increase in molecular mass and size of the molecule. The position of the first peak in the propylene carbonate RDF at 5.3 Å determined here at 298 K (Figure 4) compares favourably with earlier MD simulation and X-ray scattering studies, recorded at 323 K, by Soetens *et al.* [16] where a first inter-molecular peak in the total structure function of propylene carbonate was reported at *ca.* 6 Å.

Since the RDFs of both propylene carbonate and glycerol carbonate were essentially identical, to understand how the two solvents differ in their liquid structure at the atomic scale, we needed to examine and compare their specific site-site interactions. These revealed some significant differences in the local liquid structure correlations of propylene carbonate and glycerol carbonate, that were not evident from the centre of mass RDFs. These inter-molecular correlations can be examined by reference to the full-range of specific site-site partial radial distribution functions (pRDFs), and are discussed below.

Propylene carbonate

Two potentially important interaction modes have been identified in propylene carbonate from MD and QM modelling. Small cluster QM calculations[18] identified the presence of weak intramolecular O···H-C hydrogen-bonding interactions as a key signature. In contrast, Silva and Freitas[19] interpreted C···O and O···O correlations observed in larger ensem-

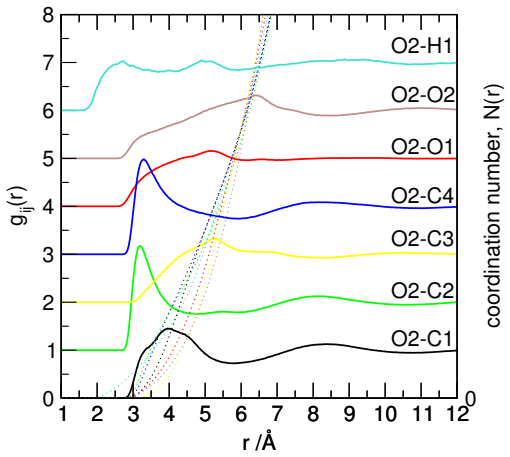

Fig. 5 Site-site pRDFs (solid lines) and the corresponding coordination numbers (dotted lines) from the carbonyl oxygen atom (O2) of propylene carbonate. The marked correlation between the carbonyl O2 oxygen and the C2 and C4 atoms of the propylene fragment is revealed by the distinct maxima in the pRDFs at *ca.* 3.5 Å and, in contrast, only weak diffuse correlations between oxygen sites are evident.

ble Monte Carlo simulations in terms of the presence of head-to-tail propylene carbonate dimers, an explanation first used by Eckstein *et al.* [17] to rationalise orientational pair correlations obtained from molecular simulation and X-ray scattering. MD simulation coupled with sum frequency generation spectroscopy[28] supports the formation of head-tail propylene carbonate dimers at the liquid surface in contrast to dimethyl carbonate, for which a random interfacial structure was observed.

EPSR simulation derived site-site pRDFs (solid lines) and the corresponding coordination numbers (dashed lines) from the carbonyl oxygen atom of propylene carbonate (O2) are shown in Figure 5. The full suite of pRDFs between oxygen and carbon atoms are included in Figures S1-6 in the ESI.†

A first peak in the O2-H1 pRDF can be observed from 1.8 Å showing a maximum at 2.5 Å and a second at 5 Å. This correlation is a clear indicator of intermolecular interactions. However, because propylene carbonate is modelled here with all the hydrogen atoms defined as the same type (H1) due to the limited positional H/D substitution available from the experimental samples, this correlation pRDF scans all the carbonyl···hydrogen correlations in the system. The carbonyl oxygen O2···O2 intramolecular distribution function appears similar to that from Soetens *et al.* [16] with a small shoulder around 3 Å followed by a steady increase in the probability density to a maximum at *ca.* 6.5 Å. We note that this site-site peak maxima is at a greater correlation length than that of the first peak in RDF. The intermolecular pRDFs between the carbonyl oxygen and carbon atoms (C1, C2, and C4) display much more pronounced peaks at 3.2 Å (O2···C2), 3.3 Å (O2···C4) and 4.0 Å (O2···C1) compared to O2···O2. The O2···C1 peak is broader and occurs at a longer

distance than those between O2 and C2/4. This longer correlation distance to the C1 site appears to be geometrically related to the correlations to C2 and C4. The small shoulder at 3.5 Å indicates that the carbonyl group can approach this carbon site. The remaining correlations to the carbonyl oxygen atom (O2···O1 and O2···C3) appear as broad, poorly defined humps around the averaged COM correlation distance of the first shell at *ca.* 5.5 Å.

Running coordination numbers for each of the site-site distribution functions considered above are also included in Figure 5. It is notable that within the first coordination shell, the O2···Cn (n = 1, 2, 4) correlations from the carbonyl oxygen to propylene carbon atoms have coordination numbers of 3.5 at 5 Å, which are larger than those for O2···O2 and O1 (2.2 at 5 Å). The coordination numbers for all these first shell correlations converge to values of *ca.* 6, as the correlation distance approaches 6.2 Å.

Both the overall average coordination numbers determined from the RDFs of 2.7 at 5.0 Å increasing to 5.9 at 6.0 Å and with MD calculations on bulk liquid propylene carbonate (2.5 at 5.0 Å, increasing to 6.0 at 6.0 Å).[22] Similarly, the C···O and O···O pRDFs in Figure 5 are consistent with results from Monte Carlo simulations.[19] The dominant O2···C correlations in both studies are also consistent with small cluster calculations of Wang and Balbuena[18] where specific intermolecular O···H-C hydrogen-bonding interactions were identified.

Thus, the results from neutron scattering appear compatible with simulation data supporting both head-to-tail dimer and C=O···H-C hydrogen-bonding association modes. However, the C3···C3 pRDF, which has a broad maximum at 5.6 Å shows no correlation probability below 3.8 Å. This contrasts to the recent surface simulations of Wang *et al.*[28] who identified dimers with an optimal C3···C3 separation of 3.4 Å.

Glycerol carbonate

The pRDFs for the carbonyl and hydroxyl oxygen sites (O2 and O3 respectively) of glycerol carbonate are shown in Figure 6, additional oxygen and carbon centred pRDFs are included in Figures S7-12 in the ESI.†

Compared to the corresponding pRDFs for propylene carbonate, the correlations here are much less well defined. The O2···C2/4 correlations for example, that in propylene carbonate are responsible for the strong head-to-tail chain association in the liquid, now occur at 3.5 Å as much smaller peaks with significantly reduced intensity. Also, notably, the O2···C1 distribution function, which occurred as a broad hump ranging from 3–5 Å with a maximum at 4.0 Å for propylene carbonate, shows a much more pronounced shoulder at 3.5 Å indicating close contact correlations, and a second peak at *ca.* 4.5 Å.

The greatest changes in the carbonyl environment of glycerol carbonate are associated with pronounced carbonyl-carbonyl and carbonyl-hydroxyl correlations (O2···O2 and O2···O3) that occur at short distances with peaks in the pRDFs at 3.0 Å. Associated with

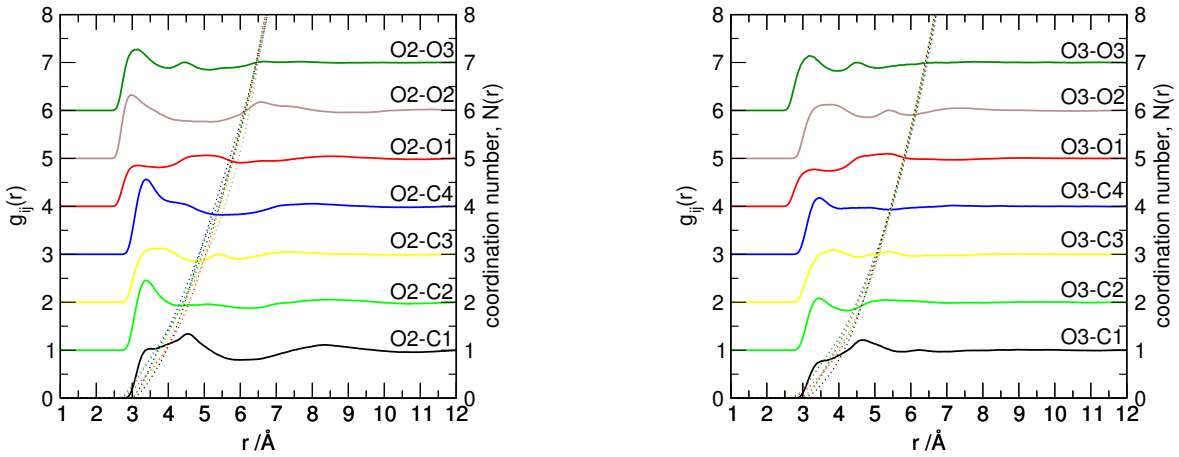

Fig. 6 Site-site pRDFs (solid lines) and the corresponding coordination numbers (dotted lines) from the carbonyl oxygen atom (O2) (left) and alcohol oxygen (O3) (right) of glycerol carbonate. Compared to the pRDFs of propylene carbonate in Figure 5, a marked increase in oxygen···oxygen correlations is evident.

this increased proximity of carbonyl pairs is an enhancement in the O2···C3 pRDF which is evident as a broad peak at 3.7 Å (3.3–4.2 Å) contrasting with the propylene carbonate case. The short carbonyl–carbonyl O2···O2 correlation in glycerol carbonate (3.0 Å) in contrast to the case for propylene carbonate (maximum at 6.5 Å). This is the most profound indicator of major differences in the liquid structures of these two cyclic carbonates. Correlations to the hydroxyl O3 oxygen centre (Figure 6) show similar behaviour to those from O2, again with significantly smaller peaks at the first maximum in the pRDFs. First maxima are observed as small peaks between 3.0–3.5 Å between O3 and all the other non-hydrogen atoms in the system (C1-4 and O1-3) with little to distinguish between the different site-site correlations.

Comparing the running coordination numbers for correlations to the O2 and O3 sites in glycerol carbonate (shown in Figure 6), there are no major differences between individual pRDFs, with coordination numbers that average 3.0 to 5.0 Å increasing to 6.0 by 6.0 Å. This contrasts with propylene carbonate where O2···C2/4 correlations exhibited higher coordination numbers in the first contact shell than those from O2···O1 and O2···C3. When taken with the relatively small sizes of the first peaks in the pRDFs in Figure 6, this indicates that glycerol carbonate has a more homogeneous structure with less orientational preference than propylene carbonate. In which case, the apparently high O2···O2 and O2···O3 correlations may be a consequence of the positions of these atoms at the extremes of the glycerol carbonate molecule.

The hydroxyl-group present in glycerol carbonate has been cited as a source of water-like behaviour compared to propylene carbonate.[5,15] and it was anticipated that this functional group would provide an important positive contribution to the overall structure of

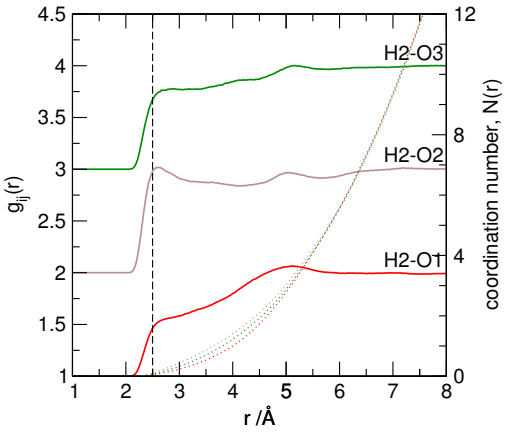

Fig. 7 Site-site pRDFs (solid lines) and the corresponding coordination numbers (dotted lines) from the alcohol H2 atom of glycerol carbonate. Notably, the H2···O2 correlation at 2.6 Å is greater than that in the corresponding H2···O3 pRDF, signifying a greater distribution of alcohol–carbonyl interactions at the cost of alcohol–alcohol interactions.

the liquid, as is found in the simple alcohols.[29]

However, examining the three hydroxyl H2···oxygen pRDFs in glycerol carbonate (Figure 7), prominent peaks are not observed with all three pRDFs showing only a small peak (H2···O2) or shoulder (H2···O1 and H2···O3) at 2.5 Å. If this correlation distance is interpreted in terms of hydrogen bonding, then this is a long *'moderate, mostly electrostatic'* association[30] and it is notable that the most pronounced H2···oxygen correlation is to O2 and not to O3. The H2···O3 coordination number, calculated to 2.5 Å, was 0.49 ± 0.55. This contrasts both simple alcohols such as methanol[31] where 0.99 ± 0.06 hydrogen bonds to 2.36 Å (and 2.02 ± 0.02 to 2.78 Å) were reported, and to polyols such as glycerol.[32] In the glycerol case, hydrogen bond analysis revealed 0.96 ± 0.61 O–H to the terminal hydroxyl oxygen of glycerol and 0.62 ± 0.63 for the central hydroxyl oxygen, this is evidence that hydroxyl···hydroxyl hydrogen-bonding is much less of a dominant structure-forming interaction in glycerol carbonate, and that it is unlikely that 'water-like' domains form and percolate through the solvent. In contrast these pRDFs suggest that only weak hydroxyl–hydroxyl inter-molecular hydrogen bonding may be present in neat glycerol carbonate and that the most significant interactions of the hydroxyl group are non-directional spatial correlations with the carbonate oxygen-sites. It is these interactions that lead to a disruption of the preferred polar correlations of carbonyl C=O groups to the ring that are found in propylene carbonate.

Local spatial structure correlations

The spatial relationship between near-neighbour sites can be highlighted by examining spatial density functions (SDFs). For both propylene carbonate and glycerol carbonate, SDFs between the carbonyl group (C3=O2) and molecular centre-of-mass (COM) were calcu-

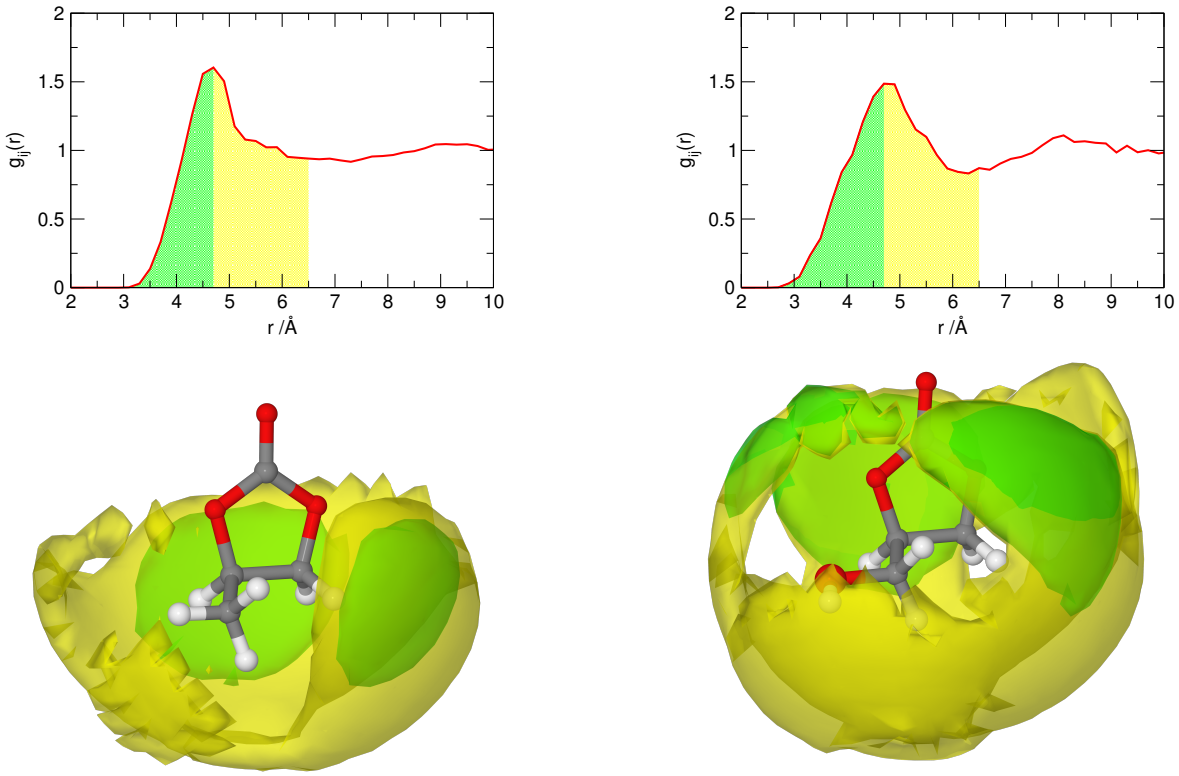

Fig. 8 Carbonyl–COM pRDFs for propylene carbonate (top left) and glycerol carbonate (top right) and the corresponding SDF surfaces (bottom) showing the top 25% probability density for correlations of carbonyl croups to the molecular centre of mass of a molecule within the distance limits 3.0–4.7 Å (green, short distance correlations leading to the maximum in the first shell) and 3–6.5 Å (yellow, encompassing all first shell correlations to 6.5 Å). For propylene carbonate (left) a marked interaction between the carbonyl groups and ring-H atoms of the central molecule is clearly evident, whereas for glycerol carbonate (right), the corresponding short distance correlation is more disperse and associated with carbonyl–oxygen atoms of the cyclic carbonate ring rather than carbonyl–ring hydrogen sites.

lated. Figure 8 shows the pRDF for the C=O···COM correlations (top) and the corresponding SDF (bottom) plotting the top 25% probability density within the first coordination shell around the molecules. The distribution of correlations upto the peak maxima in the first correlation shell (at 4.7 Å) and within the complete first shell (to 6.5 Å) are plotted. The corresponding COM–COM SDFs plotted to show both the top 25 % and 5 % probability densities over the same first shell region (3.0–6.5 Å) are included in Figure S13 of the ESI† and show show similar, diffuse distributions of molecules within the first correlation shell. The highest probability correlations (top 5 % probability) occur as a broad band above and below the ring of the molecules.

In contrast to the largely isotropic appearance of the COM–COM SDFs, the carbonyl–COM SDFs (Figure 8) show marked differences in the carbonyl correlation position around

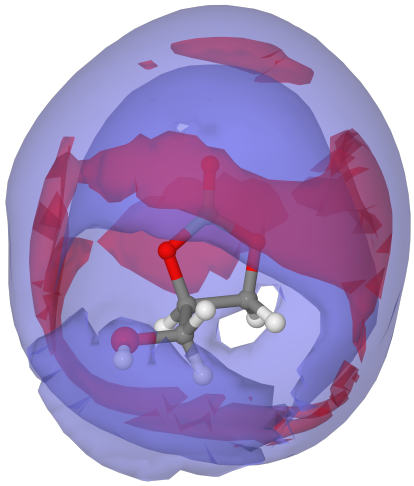

Fig. 9 Glycerol carbonate –OH to COM SDFs derived from the EPSR model showing the diffuse and non-specific correlations of the hydroxyl function of glycerol carbonate. The SDFs are plotted to show the top 25 % (blue) and 5 % (red) density surfaces corresponding to interactions plotted within the first coordination shell (3–6.5 Å).

a central molecule compared with the averaged probability distributions of molecules within the coordination shell (as seen in the COM SDF). Additionally, there are significant differences in the carbonyl–COM SDFs between propylene carbonate and glycerol carbonate. For propylene carbonate, the greatest contributions to short distance correlations are carbonyl group hydrogen-bonding associations with ring C–H hydrogen positions on both sides of the propylene carbonate ring. These short (3.0–4.7 Å) correlations are shown in green in Figure 8. Exploring the carbonyl-COM correlations over longer distances, up to 6.5 Å (the minimum in the pRDF), the SDF expands to form an approximate hemisphere encompassing the three carbon atoms and their associated hydrogens. This is consistent with the strong correlations in the O2–C*n* pRDFs. Notably, there is no regions corresponding to carbonyl–carbonyl or carbonyl–O correlations are observed. The preferred organisation of propylene carbonate molecules, with strong O2···C*n* correlations (show in the pRDFs in Figure 5) and the absence of significant C3···C3 correlations at distances less than 5.3 Å is consistent with the hydrogen-bonding association model described by Wang and Balbuena[18] for small molecular clusters. This suggests that, in the bulk liquid, extended networks of propylene carbonate molecules may be formed as chains with approximately collinear alignments of dipoles, as has been recently been identified for chloroform[33] rather than anti-parallel alignment as observed for acetone and dimethylsulfoxide.[34]

In contrast, the corresponding carbonyl–COM SDF for glycerol carbonate shows a different primary correlation of carbonyl groups around a glycerol carbonate molecule. The shortest correlations in Figure 5 (3.0–4.7 Å, green) correspond to carbonyl–carbonate interactions above/below the CO_3 triangular apex of the ring. A more diffuse correlation

environment is evident over the total first shell to 6.5 Å than for propylene carbonate with correlations evident associated with both the hydrogen sites *and* carbonate regions of the molecule.

Clearly, the presence of the hydroxyl group in glycerol carbonate leads to significant disruption of the C=O···H–C hydrogen-bonding motif seen in propylene carbonate. Short distance correlations between the hydroxyl O3 site and all other oxygen sites in the molecule have been described earlier, and are shown as site-site pRDFs in Figure 6. Calculating the SDF of the glycerol carbonate hydroxyl–COM correlation using the same criteria as were used for the carbonyl–COM correlations (top 25 % probability density between 3–6.5 Å), an extremely broad, diffuse and undefined spatial distribution can be observed with a close to isotropic distribution of the hydroxyl groups around a central glycerol carbonate molecule is observed (Figure 9). This broad distribution is consistent with the hydroxyl group having a destructuring effect on the liquid, with the multiple weak non-specific hydrogen-bonding interactions competing with C=O···C2/4 aggregation modes present in propylene carbonate. The net effect of which is to generate a more disordered liquid without structure directing interactions. Even when the top 5 % of the correlation density is examined (Figure 9), a relatively broad distribution of correlation sites including positions that appear associated with the hydroxyl O3, carbonyl O2, and O1 oxygen sites through correlation above/below the ring can be identified.

Bulk structure correlations in the two liquids

There is significantly greater spatial correlation evident in the carbonyl-COM SDF of propylene carbonate compared to glycerol carbonate (Figure 8). For propylene carbonate, the high C=O···C2/4 interaction probability leads to the formation of correlated head-to-tail chains of molecules in the liquid due to the preferred formation of hydrogen-bonds between hydrogen atoms of propylene moieties to the O2 oxygen of the carbonyl group of adjacent molecules in the first coordination sphere. This is a consequence of the dipole moment along the carbonyl group of propylene carbonate which leads to polarisation with $\delta+$ hydrogens and a $\delta-$ partial charge on the carbonyl O2 site.

Percolation of these strong positional hydrogen-bonding correlations should result in the formation of molecular chains or clusters within the liquid. The correlation length was calculated using the 'chain' distribution routine in ESPR for C=O···propylene group associations. The average number of chain-forming correlations per molecule and average chain lengths are shown in Table 4 for each of the defined cut-off distances. Using a short distance criteria (3.50 Å), the average number of correlations contributing to chains is 0.41 per propylene carbonate molecule with 66% of the molecules not exhibiting any C=O···C2/4 correlations within the cut-off criteria and 28% only having one correlation. When the cut-off was extended to 3.75 Å, 74% of propylene carbonate molecules become involved in at least one C=O···C2/4 interaction with 36% involved in two or more chain-

forming correlations. As the acceptance cut-off is increased from 3.5–4.0 Å, the average number of chain-forming correlations increases. Using a 4.00 Å cut-off, 91% of propylene carbonate molecules participate in two or more C=O···C2/4 chain-forming correlations (*i.e.* forming head-to-tail chains).

The average chain correlation length, calculated from the correlation populations, for propylene carbonate shows a marked maximum distribution at around 20 Å using the 4.00 Å chain-forming limit (Figure 10). This suggests that propylene carbonate forms chains with correlation lengths that average 4–5 molecules (molecular cross section of propylene carbonate is approximately 5.4×3.2 Å).

In contrast, the more diffuse carbonyl– and hydroxyl–COM SDFs of glycerol carbonate in Figures 8 and 9 indicate a less tightly structured liquid with a first coordination sphere which is poorly defined. The corresponding chain-forming correlation calculations were carried out for glycerol carbonate taking into account (i) C=O···C3/4 correlations consistent with the head-to-tail stacking in propylene carbonate, (ii) C=O···H-O3 correlations (carbonyl to $-CH_2OH$) and (iii) either C=O···O=C or C=O···H-O3 correlations (associations at the contact limit with no net preferred directional orientation). The results are also shown in Table 4 and Figure 10.

Considering only the *syn*-dipolar C=O···C2/4 interaction, the average number of chain forming correlations for glycerol carbonate is $<$0.20 compared to 0.40 for propylene carbonate with the 3.50 Å limit. This increases to 1.5 when the cut-off limit is extended to 4.0 Å, however this is still lower than the average 2.11 chain forming correlations in propylene carbonate and the majority of glycerol carbonate molecules only participate in one carbonyl to ring association. Adding in associations of the carbonyl group with the alcohol C=O···CH_2OH region of the molecule, the number of chain forming correlations increases although at the short 3.50 Å cut-off is still lower than for propylene carbonate (note, in Table 4 the C=O···C4 correlation is counted twice). When both *anti*-dipolar C=O···O=C and *syn*-dipolar C=O···H–O3 associations are counted as chain-forming, then an average of 0.65 chain forming O···O correlations per glycerol carbonate molecule are obtained at the 3.5 Å cut-off. This is indicative of the much lower orientational molecule–molecule correlation in which the carbonyl group experiences a coordination environment containing a range of different atomic sites resulting in the formation of a dispersed liquid environment with little supra-molecular structuring. The average chain correlation length, calculated for glycerol carbonate, supports this picture. Using the 4.00 Å correlation cut-off limit, the greatest number of molecules participated in only one chain-forming 'head-to-tail' correlation. However, the chain length distribution populations (N_{CL}) is broadly consistent across the entire range of chain correlation lengths (Figure 10) indicating a lack of specific aggregation.

Table 4 Average number (N_{AV}) of chain-forming correlations and average chain length (N_{CL}) with standard deviations from the EPSR 'chains' sub-routine for propylene carbonate and glycerol carbonate.

	D/Å	N_{AV}	N_{CL}/Å
Propylene carbonate			
C=O···C2/4	3.50	0.40 (0.60)	1.27 (0.65)
	3.75	1.23 (0.96)	5.83 (5.78)
	4.00	2.11 (1.16)	19.96 (5.32)
Glycerol carbonate			
C=O···**C2/4**	3.50	0.17 (0.41)	1.10 (0.34)
	3.75	0.72 (0.80)	1.77 (1.44)
	4.00	1.50 (1.10)	22.78 (14.53)
C=O···**C**H_2**O**H	3.50	0.18 (0.41)	1.10 (0.35)
	3.75	0.77 (0.81)	1.95 (1.72)
	4.00	1.60 (1.12)	27.67 (12.17)
C=O···**O**=C	3.50	0.64 (0.76)	1.62 (1.25)
and	3.75	1.22 (1.01)	8.54 (7.98)
C=O···H**O**CH_2	4.00	1.91 (1.23)	20.23 (6.01)

Conclusions

Experimental neutron scattering data has been collected for a range of H/D isotopically substituted samples of propylene carbonate and glycerol carbonate at 25 °C. Although the radial distribution functions for the two liquids are very similar, significant differences in the local structure correlations are observed from EPSR modelling of the data. Propylene carbonate exhibits a strong orientational correlation in the liquid state generated by C=O···H−C 'head-to-tail' hydrogen-bonding forming chains with a broad distribution and mean length of 20 Å, corresponding to 4–5 molecules. This organisational structure is consistent with the small cluster QC models of Wang and Balbuena[18] and with the general interpretation of MD/X-ray studies[16] and Monte Carlo simulations[19] but bring greater clarity to the organisation of the molecules in the liquid state that has not been explored in subsequent MD studies.[20]

For glycerol carbonate, an emerging bio-sourced solvent and chemical intermediate, no previous structural studies have been reported. Hydrogen-bonding from the terminal –OH group of glycerol carbonate was anticipated to contribute significantly to differences in the structures of glycerol carbonate and propylene carbonate, with an expectation that hydrogen-bonded networks, as seen for glycerol[32] and small alcohols, would be observed. However the results obtained suggest that the primary effect of the hydroxyl group is to disrupt the structuring forming 'head-to-tail' C=O···C2/4 aggregation motif present in propylene carbonate, with the net effect of generating a disordered liquid with no overall

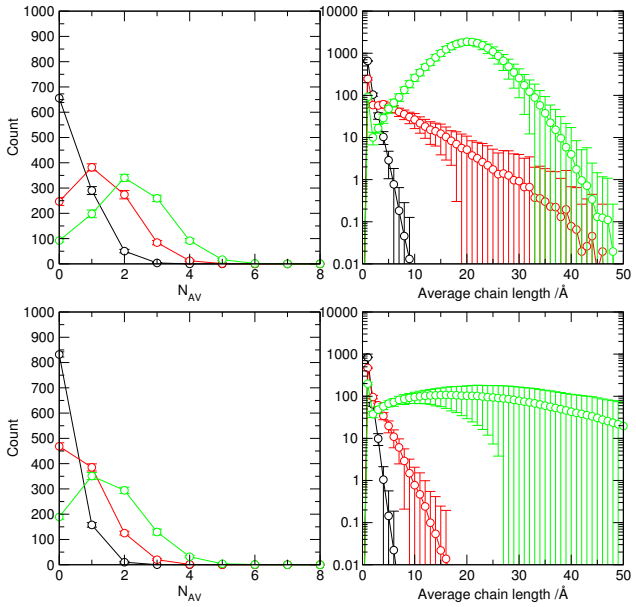

Fig. 10 Results from the 'chains' analysis routine in EPSR for propylene carbonate (top) and glycerol carbonate (bottom) based on the criteria of a C=O···C2/4 correlation distance of less than 3.5 (black), 3.75 (red) or 4.0 Å (green), showing (left) the average number of chain-forming correlations per molecule (N_{AV}) and (right) the average chain length (N_{CL}).

structure directing interactions.

Acknowledgements

We acknowledge Green Lizard Technologies Ltd and QUILL for PhD studentships to YD and MG respectively, the Science and Technology Facilities Research Council (STFC) for beamtime on SANDALS (ISIS experiment RB1610258) and Dr S. K. Callear (ISIS) for support with the experiments.

References

1 A. A. G. Shaikh and S. Sivaram, *Chem. Rev.*, 1996, **96**, 951–976.

2 B. Schaeffner, F. Schaeffner, S. P. Verevkin and A. Boerner, *Chem. Rev.*, 2010, **110**, 4554–4581.

3 L. Simeral and R. L. Amey, *J. Phys. Chem.*, 1970, **74**, 1443–1446.

4 (*a*) S. A. Freunberger, Y. Chen, Z. Peng, J. M. Griffin, L. J. Hardwick, F. Barde, P. Novak and P. G. Bruce, *J. Am. Chem. Soc.*, 2011, **133**, 8040–8047; (*b*) V. Etacheri, R. Marom, R. Elazari, G. Salitra and D. Aurbach, *Energy & Env. Sci.*, 2011, **4**, 3243–3262.

5 M. O. Sonnati, S. Amigoni, E. P. T. de Givenchy, T. Darmanin, O. Choulet and F. Guittard, *Green Chem.*, 2013, **15**, 283–306.

6 Y. Chernyak, *J. Chem. Eng. Data*, 2006, **51**, 416–418.

7 J. H. Clements, *Ind. Eng. Chem. Res.*, 2003, **42**, 663–674.

8 J. F. Knifton and R. G. Duranleau, *J. Mol. Catal.*, 1991, **67**, 389–399.

9 M. Pagliaro and M. Rossi, *The Future of Glycerol: Edition 2*, The Royal Society of Chemistry, 2010, pp. P001–P170.
10 J. R. Ochoa-Gómez, O. Gómez-Jiménez-Aberasturi, B. Maestro-Madurga, A. Pesquera-Rodríguez, C. Ramírez-López, L. Lorenzo-Ibarreta, J. Torrecilla-Soria and M. C. Villarán-Velasco, *Applied Catalysis A: General*, 2009, **366**, 315–324.
11 G. Rokicki, *Prog. Polym. Sci.*, 2000, **25**, 259–342.
12 M. L. Maminski, P. G. Parzuchowski, A. Trojanowska and S. Dziewulski, *Biomass & Bioenergy*, 2011, **35**, 4461–4468.
13 (*a*) T. Mizuno, T. Nakai and M. Mihara, *Heteroat. Chem.*, 2010, **21**, 99–102; (*b*) T. Mizuno, T. Nakai and M. Mihara, *Heteroat. Chem.*, 2010, **21**, 541–545.
14 (*a*) G. Ou, B. He and Y. Yuan, *Appl. Biochem. Biotechnol.*, 2012, **166**, 1472–1479; (*b*) G. Ou, B. He and Y. Yuan, *Enzyme Microb. Technol.*, 2011, **49**, 167–170.
15 (*a*) S. P. Porras, M. L. Riekkola and E. Kenndler, *Electrophoresis*, 2003, **24**, 1485–1498; (*b*) J. Muzikar, T. van de Goor, B. Gas and E. Kenndler, *Anal. Chem.*, 2002, **74**, 428–433.
16 J. C. Soetens, C. Millot, B. Maigret and I. Bako, *J. Mol. Liq.*, 2001, **92**, 201–216.
17 E. Eckstein, J. Qian, R. Hentschke, T. Thurn-Albrecht, W. Steffen and E. W. Fischer, *J. Chem. Phys.*, 2000, **113**, 4751–4762.
18 Y. Wang and P. B. Balbuena, *J. Phys. Chem., A*, 2001, **105**, 9972–9982.
19 L. B. Silva and L. C. G. Freitas, *J. Mol. Structure*, 2007, **806**, 23–34.
20 (*a*) P. Ganesh, D.-E. Jiang and P. R. C. Kent, *J. Phys. Chem. B*, 2011, **115**, 3085–3090; (*b*) S. Lee and S. S. Park, *J. Phys. Chem. B*, 2011, **115**, 12571–12576; (*c*) X. You, M. I. Chaudhari, S. B. Rempe and L. R. Pratt, *J. Phys. Chem., B*, 2016, **120**, 1849–1853.
21 Y. Kameda, Y. Umebayashi, M. Takeuchi, M. A. Wahab, S. Fukuda, S. Ishiguro, M. Sasaki, Y. Amo and T. Usuki, *J. Phys. Chem., B*, 2007, **111**, 6104–6109.
22 O.-S. Lee and M. A. Carignano, *J. Phys. Chem. C*, 2015, **119**, 19415–19422.
23 R. Nagumo, Y. Muraki, M. Taniguchi, H. Furukawa, S. Iwata, H. Mori and H. Takaba, *J. Chem. Eng. Jpn.*, 2016, **49**, 1–5.
24 G. Rokicki, P. Rakoczy, P. Parzuchowski and M. Sobiecki, *Green Chemistry*, 2005, **7**, 529–539.
25 A. K. Soper, *GudrunN and GudrunX: Programs for correcting raw neutron and X-ray diffraction data to differential scattering cross section, RAL-TR-2011-013*, Rutherford Appleton Laboratory technical report, 2011.
26 A. K. Soper, *Chem. Phys.*, 1996, **202**, 295–306.
27 A. K. Soper, *Mol. Phys.*, 2001, **99**, 1503–1516.
28 L. Wang, Q. Peng, S. Ye and A. Morita, *The Journal of Physical Chemistry C*, 2016, **120**, 15185–15197.
29 (*a*) Y. Yamaguchi, K. Hidaka and A. K. Soper, *Mol. Phys.*, 1999, **96**, 1159–1168; (*b*) C. J. Benmore and Y. L. Loh, *J. Chem. Phys.*, 2000, **112**, 5877–5883; (*c*) D. T. Bowron, J. L.

Finney and A. K. Soper, *Mol. Phys.*, 1998, **93**, 531–543.
30 G. A. Jeffrey, *An Introduction to Hydrogen Bonding*, Oxford University Press, New York, 1997.
31 A. K. Adya, L. Bianchi and C. J. Wormald, *J. Chem. Phys.*, 2000, **112**, 4231–4241.
32 J. J. Towey, A. K. Soper and L. Dougan, *Phys. Chem. Chem. Phys.*, 2011, **13**, 9397–9406.
33 J. J. Shephard, A. K. Soper, S. K. Callear, S. Imberti, J. S. O. Evans and C. G. Salzmann, *Chem. Commun.*, 2015, **51**, 4770–4773.
34 S. E. McLain, A. K. Soper and A. Luzar, *J. Chem. Phys.*, 2006, **124**, 074502.